Long-range magnetic order and the Darwin Lagrangian

Vishal Mehra and Jayme De Luca
Departamento de Física, Universidade Federal de São Carlos, Rod. Washington Luiz km 235, 13565-905, Caixa Postal 676, São Carlos, SP, Brazil
(Received 30 August 1999)

We simulate a finite system of N confined electrons with inclusion of the Darwin magnetic interaction in two and three dimensions. The lowest-energy states are located using the steepest descent quenching adapted for velocity dependent potentials. Below a critical density the ground state is a static Wigner lattice. For supercritical density the ground state has a nonzero kinetic energy. The critical density decreases with N for exponential confinement but not for harmonic confinement. The lowest-energy state also depends on the confinement and dimension: an antiferromagnetic cluster forms for harmonic confinement in two dimensions.

PACS number(s): 05.70.Fh, 41.20.−q, 64.70.−p, 36.40.−c

I. INTRODUCTION

The use of fast modern computers has made it increasingly easy to investigate many-dimensional finite systems and to study dynamical quantities such as time to equipartition, symmetry break in finite systems, and quantities of thermodynamic interest [1–6]. The numerical studies have also revealed unexpected features of finite systems like cluster formation [3–5] and lack of equipartition [1,2]. In this paper we study numerically the energetic quenching of a classical electron gas with inclusion of the magnetic interaction [7–9]. The main motivation to study this system is the physics it describes and unfortunately the dynamics of this finite system is not easy to study because the equations of motion are algebraic-differential in character [10]. Because of this we explored numerically only the quenching motion, which involves integration of simple ordinary differential equations. Like the Coulomb interaction, the magnetic interaction is a long-range interaction. The long-range nature of the Coulomb interaction has been widely explored in molecular dynamics and there is a large literature of numerical simulations and various special techniques that were invented to deal with the long-range nature of the interaction [11]. On the other hand, the magnetic interaction has been much less studied.

The magnetic interaction appears naturally in classical Maxwell electrodynamics: The lowest-order retardation and magnetic effects [or order $(v/c)^2$] can be described in terms of electron variables only as a velocity-dependent interaction. This approximation was originally proposed by Darwin [12] to obtain a Lagrangian that bears his name. The Darwin Lagrangian is much used in atomic physics [13,14] where it is known as the Darwin-Breit interaction in its quantized form. The Darwin Lagrangian includes the lowest-order correction to the electric field of a moving charge and the lowest-order magnetic field (the Biot-Savart term). Apart from its traditional domain of atomic physics the Darwin Lagrangian has been used to model slightly relativistic plasmas [15–17] and even models of superconductivity and stellar magnetic fields [7]. These ideas extend the range of the Darwin Lagrangian from conventional relativistic correction: the Darwin corrections are also important in the low-energy (nonrelativistic) regime. One reason for that is to be found in the long range of the Darwin force and the fact that it is badly screened, unlike the Debye screening of the Coulomb force [18]. These two factors compensate for the weakness of the Darwin interaction at low velocities and make it a player in certain circumstances [7,8]. Last, the Darwin Lagrangian has also been used as an unfolding of the scale invariant degenerate Coulombian interaction to estimate long-time-scale dynamical effects in atomic physics [19].

It should be noted that the Darwin Lagrangian is neither Galilean or Lorentz invariant and therefore it can only be used as an approximation to a comprehensive relativistic physical theory [20,21]. The Darwin interaction is actually the first correction to the Coulomb interaction in both Maxwell's electrodynamics and in the relativistic action-at-a-distance electrodynamics [22]. (The series expansion for the action-at-a-distance electrodynamics is made from the usual Page series of Maxwell's theory [23] by dropping the odd powers.) Approximation is always necessary, as the exact treatment of relativistic many-body dynamical systems involves nonlocal delayed interactions that are hard to implement numerically, with some few exceptions found by Kerner and Currie that can be both Galilean and Lorentz invariant as well as local in phase space all at once [20]. The way we justify the Darwin approximation in the present work is that we operate in a reference frame (the center of mass) where all the electrons have small velocities simultaneously. It is in this frame that the Darwin interaction approximately describes the correct Lorentz-invariant physical dynamics. A discussion of the broader validity of the Darwin approximation within Maxwell's electrodynamics can be found in [9].

Experimentally, aggregates of electrons with the same sign of charge can be confined for long times using suitably chosen static electric and magnetic fields and form so-called non-neutral plasmas (for a recent review see [24]). Differently from neutral plasmas (i.e., composed of electrons with both sign of charge in approximately equal numbers), the non-neutral plasmas can attain thermal equilibrium and cool to low enough temperatures to form liquid and crystal-like states. These plasmas under various confinement geometries have been extensively studied, particularly in the last decade.

Generally the interelectron interaction is taken to be Coulombic or Yukawa.

The study of the possible low-energy states of a system may shed some light on the possibility of a phase transition. We chose to study the magnetic long-range effects in a confined electron gas and in the neighborhood of its lowest-energy state. We confine a system of charged electrons in two and three dimensions by use of a background field, taken either to be of a harmonic or exponential form. The electrons interact by Coulomb plus Darwin forces. For the purely Coulombian repulsion, it is known that the lowest-energy state of this system is a Wigner lattice (triangularlike in two dimensions), which we also find with our quenching techniques [25,26]. We show that the long-range effects depend on N and on a single parameter β, which is usually of the order of $10^{-1}-10^{-3}$ for attainable physical densities. We find that low-N systems need an artificially larger value of β for the long-range effects to be important. The assumption is that the critical value goes down with N, and because of the practical impossibility of simulating systems with millions of electrons, we investigate finite systems for an artificially higher value of β and extrapolate the scaling properties to the large-N case. This assumption holds for the exponential confinement but not for the harmonic confinement, where the critical β does not go down with N.

This paper is divided as follows. Section II introduces the model and defines the quenching procedure. The numerical results for the two-dimensional (2D) systems are described in Sec. III; two subsections correspond to types of confining potential. Section IV deals with the three-dimensional (3D) systems, again divided into subsections. The papers ends with a discussion in Sec. V.

II. DARWIN LAGRANGIAN AND THE NATURAL QUENCHING

We consider N electrons in two or three dimensions interacting via the Coulomb repulsion plus the velocity-dependent Darwin magnetic interaction [9,12] and confined by a one-electron potential $V_C(\vec{r})$ of the positive background. The Lagrangian for this system can be written as

$$L=\frac{m}{2}\sum_{i=1}^{N}\vec{v}_i^{\,2}-e^2\sum_{i<j}^{N}\frac{1}{r_{ij}}+e^2\sum_{i<j}^{N}\frac{\vec{v}_i\cdot\vec{v}_j+(\vec{v}_i\cdot\hat{e}_{ij})(\vec{v}_j\cdot\hat{e}_{ij})}{2c^2r_{ij}}-\sum_i V_C(\vec{r}_i), \tag{1}$$

where $\vec{r}_i$ and $\vec{v}_i$ are the position and the velocity of the ith electron and $\vec{r}_{ij}\equiv\vec{r}_i-\vec{r}_j$, $r_{ij}\equiv|\vec{r}_{ij}|$, $\hat{e}_{ij}\equiv\vec{r}_{ij}/r_{ij}$ is the unit vector pointing from the ith to the jth electron, e is the electronic charge, and c is the velocity of light. The first term is the kinetic energy E_K of the system and the second term is the Coulomb energy. The next term is the Darwin V_D which can be expressed in terms of the vector potential $\vec{A}$ as

$$V_D=-\frac{e}{2c}\sum_i\vec{v}_i\cdot\vec{A}_i, \tag{2}$$

with

$$\vec{A}_i(r,v)\equiv e\sum_{j\neq i}\frac{\vec{v}_j+\hat{e}_{ij}(\vec{v}_j\cdot\hat{e}_{ij})}{2cr_{ij}}. \tag{3}$$

As the Lagrangian is time independent, there is an associated energy constant which evaluates to [7]

$$E=\sum_i\frac{1}{2}m\vec{v}_i^{\,2}+\frac{e}{2c}\vec{v}_i\cdot\vec{A}_i(r,v)+\sum_{i<j}\frac{e^2}{r_{ij}}+\sum_i V_C(\vec{r}_i). \tag{4}$$

Notice that this energy is *not* of the minimal coupling type

$$E=\sum\frac{1}{2}(p_i-A_i)^2+V, \tag{5}$$

which is only the case when the magnetic field is external to the system, and consequently the vector potential is velocity independent. In the present situation, because of the internal fields, the state of minimal energy is not always the zero velocity configuration anymore, as the conditions for the Bohr-Van Laufen theorem are not satisfied [9,18,27]. [This theorem states that a velocity-independent vector potential does not affect the partition function *if* the energy is of the minimal coupling form (5).]

The form of the equations can be simplified by using scaled units: a length scale, given by the average interelectron separation R, scales positions as $\vec{x}\rightarrow R\vec{x}$ (in these units the gas has a density equal to one). Time is scaled as $dt\rightarrow\omega_0 d\tau$ where $\omega_0^2\equiv e^2/mR^3$. In these units the energy scales as $E\rightarrow m(\omega_0 R)^2\hat{E}$ with

$$\hat{E}=\sum_i\frac{1}{2}\vec{v}_i^{\,2}+\sum_{i<j}\frac{1}{r_{ij}}+\beta^2\sum_{i<j}\frac{\vec{v}_i\cdot\vec{v}_j+(\vec{v}_i\cdot\hat{e}_{ij})(\vec{v}_j\cdot\hat{e}_{ij})}{2r_{ij}}+\sum_i\hat{V}_C(\vec{r}_i). \tag{6}$$

The parameter β^2 in the above equation is defined as

$$\beta^2\equiv\frac{r_e}{R}, \tag{7}$$

where $r_e=e^2/mc^2$ is the classical electron radius and the interelectronic distance R in 2D is given by $R=1/\sqrt{n}$ and $R=n^{-1/3}$ in 3D. For some real physical situations: The conduction band in metals forms a 3D degenerate plasma with typical densities of $n\sim10^{23}$ cm^{-3}, which gives for β^2 the value of $\beta^2\sim10^{-6}$. The highest density physical plasma is found in the interior of white dwarf stars, corresponding to an electron density of $n\sim10^{32}$ cm^{-3} which gives $\beta^2\sim10^{-3}$ [28].

Once the systems studied here are rotationally invariant, Noether's theorem determines a constant of motion [29] for them

$$C\equiv\sum_{i=1}^{N}\vec{r}_i\times\vec{v}_i+\beta^2\sum_{i<j}^{N}\frac{\vec{r}_i\times\vec{v}_j+(\vec{r}_i\times\hat{e}_{ij})(\vec{v}_j\cdot\hat{e}_{ij})}{2r_{ij}}, \tag{8}$$

with $\hat{e}_{ij}\equiv\vec{r}_{ij}/r_{ij}$, as before. For 2D this constant is a vector perpendicular to the plane and for 3D the O(3) symmetry

determines a constant vector by the above formula. This constant can be interpreted simply as the sum of the mechanical angular momenta plus the field angular momentum.

To look for the minimum energy states of the velocity-dependent N-body system, we adapt a numerical procedure analogous to the steepest descent quenching using what we name the natural quenching vector field. We check that for potential systems this procedure produces the static crystalline arrangement of electrons known as the Wigner lattice [25,26]. We now define the natural quenching vector field, which is constructed from the differential of the expression for the energy constant given by Eq. (6). We start from a random initial condition and integrate it as a function of a ''quenching parameter'' by the following gradient equations:

$$\frac{d\vec{r}_i}{ds} = -\frac{\partial E}{\partial \vec{r}_i}, \quad \frac{d\vec{v}_i}{ds} = -\frac{\partial E}{\partial \vec{v}_i}. \tag{9}$$

It is easy to see that along this gradient motion the energy always decreases, as the parameter derivative of the energy evaluates to

$$\frac{dE}{ds} = -\sum_i \left|\frac{\partial E}{\partial \vec{r}_i}\right|^2 - \sum_i \left|\frac{\partial E}{\partial \vec{v}_i}\right|^2. \tag{10}$$

Along with the numerical quenching from random initial conditions it is necessary to use the relativistic form of the kinetic energy. Otherwise, we observe that some electrons acquire an enormous kinetic energy during quenching, creating an enormous nonphysical internal field that still decreases the total energy. Of course, for such large velocities the Darwin approximation breaks down and the whole Lagrangian describes nonphysical effects, as discussed in Ref. [30]. In all our numerical experiments we check that the electron energies were never relativistic in the final quenched state, which guarantees that the Darwin approximation is valid. Last, to gain some understanding of how the above quenching procedure can find states with nonzero velocity, let us examine Eq. (9) for the velocities, which read as

$$\frac{d\vec{v}_i}{ds} = -\vec{v}_i - \beta^2 \sum_{j\neq i} \frac{\vec{v}_j + \hat{e}_{ij}(\vec{v}_j \cdot \hat{e}_{ij})}{2r_{ij}}. \tag{11}$$

Notice that on the right-hand side we have a linear function of the velocities, defining a linear matrix $M(\vec{r}_i, \beta^2)$. For $\beta^2 = 0$, this matrix is minus the identity and the velocities are all quenched down to zero. Above a critical value of β^2, this matrix can have negative and zero eigenvalues, and it is not possible to quench the velocities to zero anymore, which is the cause of the nonzero velocity states we find. The critical point β_c^2 can also be located by an alternative analytical method: Consider Eq. (11) for the velocity quenching. For $\beta^2 = 0$, the eigenvalues of M are all degenerate and equal to one. Taking the electron coordinates to be those of the static Wigner lattice (which can be obtained for $\beta^2 = 0$), one can diagonalize M numerically and find all its eigenvalues. The critical β_c^2 is that for which the minimum eigenvalue of M crosses zero, i.e., the minimum eigenvalue of M is just negative. It can be seen then that in this case the quenching will decrease the energy *while* increasing the velocities along the negative eigenvector directions. We have diagonalized M in the neighborhood of the Wigner lattice and it is satisfactory that the critical β^2 calculated by the matrix method agrees with the values obtained by quenching.

III. NUMERICAL RESULTS FOR CIRCULAR DISK GEOMETRY

A. Harmonic confinement

We consider first a system of N electrons in 2D, confined by the field of a uniformly charged circular disk of positive charges, of radius R_d scaled units, and with the electronic density of one electron per squared scaled unit ($N = \pi R_d^2$). For this system the potential of the uniformly charged disk of positive background can be calculated analytically [31] and for $r < R_d$ it is approximated by

$$\hat{V}_C(r) = -2\sqrt{(\pi N)} + \frac{\pi^{3/2}}{2N^{1/2}} r^2. \tag{12}$$

We have explicitly included the negative constant to properly account for the electrostatic interaction with the positive background. One still needs to add the self-energy of the positive background $\sqrt{\pi} N^{3/2}/8$ to expression (6) in order to get the total electrostatic energy. We seek to determine the lowest-energy states of this system by employing the natural quenching technique described above, and we integrate Eqs. (9) numerically with an 6/7 Runge-Kutta embedded integrator pair. By quenching from different initial conditions we can hope to obtain insight into the character of the ground state. The natural quenching is performed for the disk system for various values of the parameter β^2. The electrons are started from a triangular lattice, distorted slightly in a random manner, with velocities uniformly (and randomly) distributed up to a certain maximum value. A square-lattice-type initial configuration is also used and the same final result is found. The system is quenched until a steady state appears to have been reached. To check if we actually attain a global minimum state and not merely a local minimum, we slightly heat the obtained configuration and quench it again. By these means we are confident that our ground states are at least qualitatively correct.

These simulations are done for 225 to 1600 electrons in the disk. In all cases it is observed that below a certain value of the parameter β^2 the ground state is the static Wigner lattice, independent of the β^2. But above the critical β_c^2, a unique type of ground state is obtained. This state has nonzero kinetic energy with a striking nonuniform distribution of velocities. The electrons with large velocities are confined to an antiferromagnetic cluster in the center of the disk. The configuration in the position space remains visibly triangularlike. The electrons in the central cluster have velocities aligned in a manner to minimize the Darwin energy (Fig. 1). This parallel and antiparallel orientation of the velocities succeeds in lowering the energy of the nonstatic configuration below the static Wigner lattice.

The critical parameter value β_c^2 decreases with the increasing N, the number of electrons in the disk, but it is rather a weak dependence. For the 225 electrons disk, $\beta_c^2 \approx 0.72$ while it is approximately 0.71 for the 1600 electrons disk. The relative size of the cluster slowly decreases with

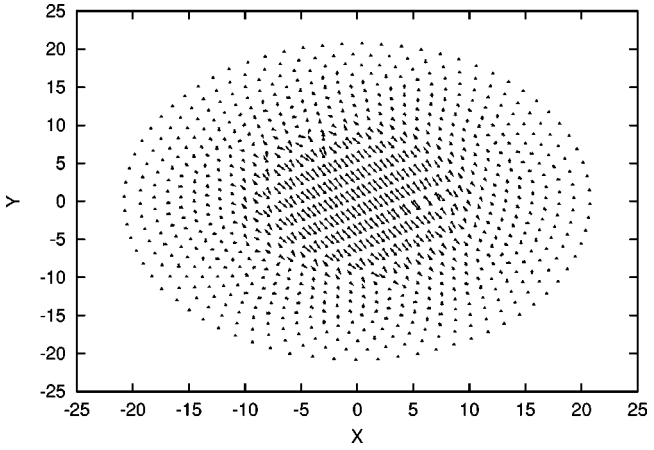

FIG. 1. The ground state of a harmonically confined disk with $N=900$ at $\beta^2=0.75$. The electrons are located at positions marked with $+$. Arrows are drawn from these positions; the length of the arrows is proportional to the magnitude of the electron velocities obtained after quenching. The direction of an arrow gives the angle of the corresponding velocity vector. Coordinates are in units of $\beta^{-2}r_e$ where r_e is the classical electron radius.

increasing N: we quantify it as following. An electron i belongs to the cluster if $\beta^2 v_i^2 > 0.01$. The quantity $\beta^2 v^2$ is generally about 0.06 for the fastest electron. At $\beta^2=0.75$, this criterion yields the fraction of the cluster electrons to be 0.31 for the 225 electron system and monotonously decreasing to 0.26 for $N=900$ and to 0.23 for $N=1600$. However, it appears that the cluster remains equally hot, independent of N, i.e., the average kinetic energy per cluster electron does not depend on N at constant β^2. Further increasing the value of β^2 beyond β_c^2 causes a rapid increase both in the size and the temperature of the cluster. The ground-state energy continues to decrease as β^2 is increased beyond β_c^2 (Fig. 2).

The quenching runs do not always yield the ground state. Often, in particular for larger-sized disks, an imperfectly aligned higher energy state is obtained. The local order is of the same type as the true ground state but on a larger scale two or more regions of the local order have a mismatch, analogous to grain boundaries in a polycrystalline material (Fig. 3).

B. Exponential confinement

The effect of choice of the confining potential may be studied by considering a different potential. To this end, we replace the harmonic potential by an exponential potential,

$$\hat{V}_C = V_0 \exp[(r-R_d)/r_W].$$

Here, as before $R_d=\sqrt{(N/\pi)}$ and $r_W=0.5$ in scaled units. The quenches are performed in a manner identical to that described above, starting from a randomly distorted triangular lattice. The critical β_c^2 is obtained, separating the static and nonstatic ground states. The values of β_c^2 are rather low and they *decrease* appreciably with increasing N. We find $\beta_c^2 \approx 0.52$ for $N=225$ to about 0.42 for $N=1600$. These (and the intermediate $N=484$ and $N=900$) values may be fitted to a power law $\beta_c^2 \sim N^{\alpha}$ with $\alpha \approx -0.11$.

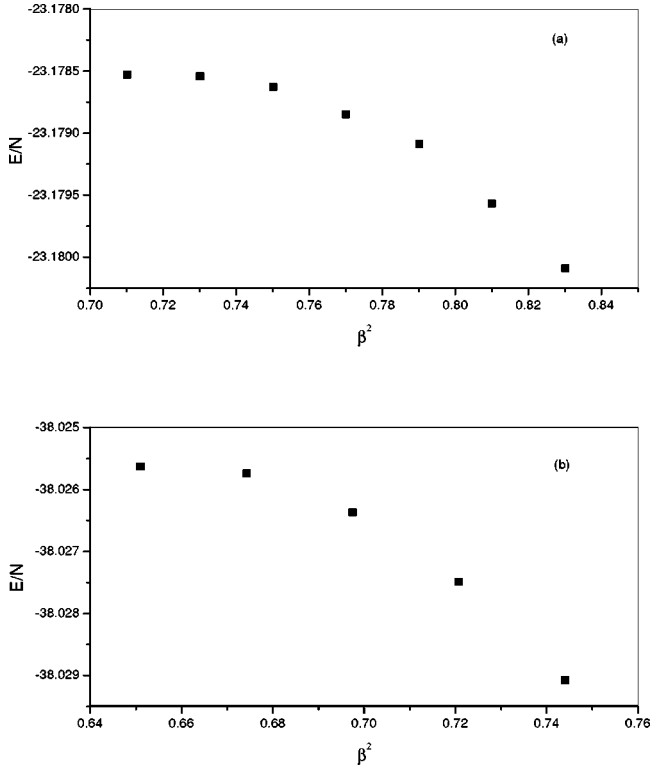

FIG. 2. (a) Ground-state energy of a harmonically confined disk with $N=225$ vs β^2. The critical β^2 is slightly less than 0.72. The energy unit is $\beta^2 e^2/r_e$. (b) Ground-state energy of a harmonically confined electron gas in 3D with $N=216$ vs β^2. The critical β^2 is slightly less than 0.67. Energy is scaled by $\beta^2 e^2/r_e$.

The character of the ground states is also affected. The edge (i.e., the surface) of the static lattice is no longer triangularlike but is composed of two ringlike layers. Above β_c^2 the velocity distribution is highly inhomogeneous: the kinetic energy is concentrated in the two edge layers (Fig. 4). Increasing β^2 beyond β_c^2 does not result in more electrons acquiring kinetic energy but merely increases kinetic energy of the edge electrons.

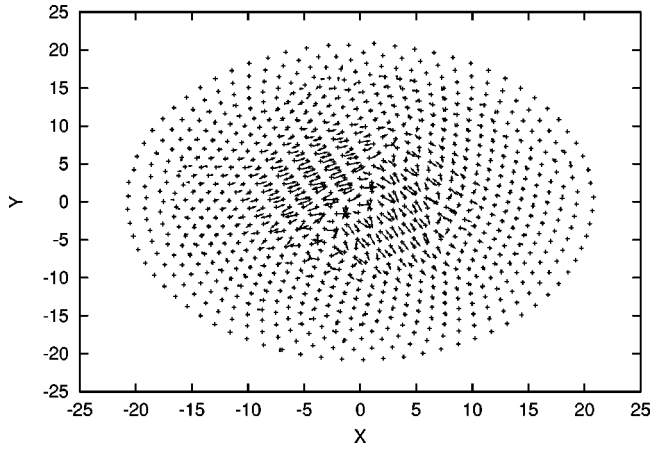

FIG. 3. A higher-energy minimum of a harmonically confined disk with $N=900$ at $\beta^2=0.75$. The arrows are made in the manner described in the previous figure. Coordinates are in units of $\beta^{-2}r_e$ where r_e is the classical electron radius.

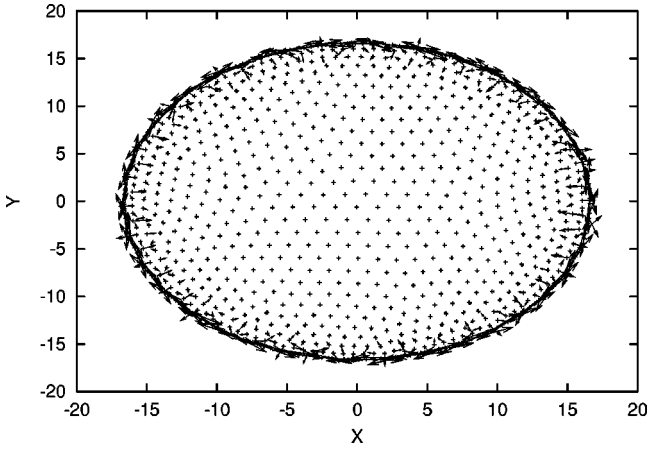

FIG. 4. The ground state of an exponentially confined electron gas in 2D at $\beta^2=0.45$. The arrows are drawn as in Fig. 1. Coordinates are in units of $\beta^{-2}r_e$ where r_e is the classical electron radius.

IV. NUMERICAL RESULTS FOR SPHERICAL GEOMETRY

A. Harmonic confinement

In this section we consider N electrons confined by the field of a homogeneous positively charged sphere of radius R_d. The potential (for $r<R_d$) can be calculated exactly,

$$\hat{V}_C=-2\pi R_d^2+\frac{2\pi}{3}r^2,$$

which follows immediately from the Gauss law of electrostatics. To obtain the total electrostatic energy we must again add the self-energy contribution of the background $(\pi/5)NR_d^2$ to expression (6). As before, the electron density is taken to be one electron per scaled unit. Quenches are performed for $N=216$–1000 electron systems. Simulations are started from a randomly distorted cubic lattice, while the velocities are initialized in the manner previously described for the disk geometry. As in the disk geometry, a critical β^2 separates static ground states from the nonstatic ground states. The critical β_c^2 is slightly smaller in three dimensions—it varies from ≈ 0.67 for $N=216$ to about 0.66 for $N=1000$.

But the character of the ground states is very different from that obtained for the disk geometry. The electrons are arranged in a multiple ringlike structure around the center of the ball. These rings possess sharp boundaries and their number grows with N. For example, the 216 electrons system has four such rings (including the cluster of central electrons) while seven rings are visible for $N=1000$ system.

This ringlike structure persists beyond β_c^2. Though, the velocity distribution is not homogeneous, a distinct cluster of hot electrons is not formed. The velocities project radially outwards (Fig. 5). The electrons in the small central cluster have smaller than average kinetic energy. The kinetic energy is fairly shared between the other rings but the distribution between electrons in a particular ring is nonuniform.

The different ordering in two and three dimensions has striking effects: in 3D the Darwin interactions between neighboring electrons are highly repulsive and the lowering of the energy is provided by the Darwin interactions of distant electrons. Whereas, in the 2D disk geometry, the Darwin interactions between nearest-neighbor electrons lower the Darwin energy.

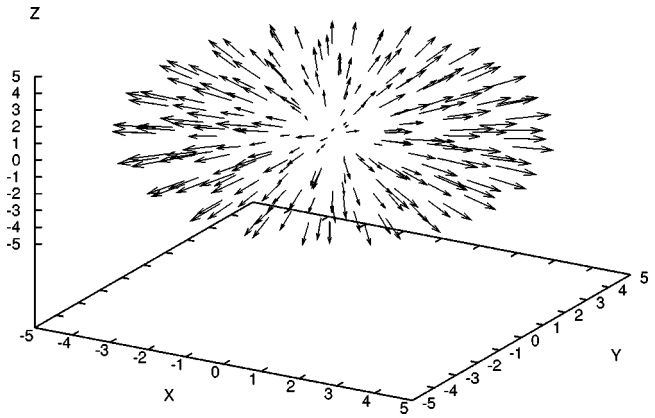

FIG. 5. The ground state for harmonically confined system in three dimensions with $N=216$ at $\beta^2=0.74$. The velocities project radially outwards. Arrows are made in a manner similar to the two-dimensional case but without pluses. Coordinates are in units of $\beta^{-2}r_e$ where r_e is the classical electron radius.

B. Exponential confinement

In this section we describe the results of the simulation of 3D electron gas confined by an exponential potential

$$\hat{V}_C=V_0\exp[(r-R_d)/r_W].$$

Here R_d is defined by the relation $N=(4\pi/3)R_d^3$, and $r_W=1.5$. The static and nonstatic ground states are again obtained, below and above β_c^2, respectively. Though, in contrast to the harmonic confinement, the β_c^2 decreases with increasing N with the power law $\beta_c^2\sim N^{-0.23}$. The values of β_c^2 range from 0.74 for $N=216$ to 0.50 for $N=1000$.

The lattice has a ringlike structure again but with some differences. First, the number of rings is smaller: $N=1000$ system has only four rings compared with seven with harmonic potential. Second, the central cluster is absent. The distribution of kinetic energy is also different from the harmonic case. The kinetic energy per electron increases as one goes outwards and for $N=1000$ the inner two rings have almost no kinetic energy.

V. DISCUSSIONS AND CONCLUSIONS

It would be natural to integrate the supercritical symmetry-breaking states of low energy and nonzero angular momentum to see the time dependence of the angular momentum [6], but this is not an easy numerical job. The existence of zero and negative eigenvalues of M in Eq. (11) signals the onset of complex dynamical behavior for this system: The Lagrangian equations of motion that follow from Eq. (1) are

$$\vec{a}_i+\beta^2\sum_{j\neq i}\frac{\vec{a}_j+\hat{e}_{ij}(\vec{a}_j\cdot\hat{e}_{ij})}{2r_{ij}}$$
$$=-\frac{dV_C}{d\vec{r}_i}-\sum_{j\neq i}\frac{\hat{e}_{ij}}{r_{ij}^2}+\beta^2\sum_{j\neq i}\frac{1}{2r_{ij}^2}\{(\vec{v}_i\cdot\hat{e}_{ij})\vec{v}_j$$
$$+[|\vec{v}_j|^2-3(\vec{v}_j\cdot\hat{e}_{ij})^2-2\vec{v}_i\cdot\vec{v}_j]\hat{e}_{ij}\}. \qquad (13)$$

Notice that this is an algebraic-differential equation [10], and the linear matrix sitting on the left side is the same exact matrix M that appeared in Eq. (11). The numerical procedure to integrate this equation is delicate: If the matrix is nondegenerate, which is the case for low values of β, the integrator RADAU [32] can be used in a fast and efficient way. If the matrix has only one zero eigenvalue, the integrator DASSL [10] can be used, as long as the matrix does not lose rank along the trajectory, which is the case for rare initial conditions only. The general high-index case where the matrix's rank is lesser than $2N-1$, or even worse if it loses rank along the trajectory, then one is faced with a rich system and certainly a very complex dynamics. As a matter of fact, in 1976 one of the earliest studies of this many-body system declared it intractable [15] and a coarse-grained field approximation was developed to study it, which later became a plasma simulation technique [17]. We could integrate initial conditions with a very low β, and there we found that the angular momentum is an approximate constant, as it should be for the $\beta=0$ case, according to Eq. (8). For intermediate values of β we are able to perform the numerical integration of the dynamics using RADAU, and we find that the total angular momentum does not change sign for very-long-time scales. In the supercritical situation, where it would be of interest to study the dynamics, we find that the time steps of RADAU quickly go to zero due to the criticality of the matrix. An integration method has still to be developed to simulate this interesting dynamics in the high algebraic index situation.

Our numerical results definitely show that for *finite N* the magnetic interaction lowers the energy below the Wigner lattice, which is the main result of this paper. The thermodynamic limit is a more subtle question, which we cannot completely decide with numerics. As regards the extensivity of the purely Coulomb lattices (undercritical densities), our results are as follows: In three dimensions, our data show that E/N tends to a constant value. This is in agreement with Gauss's law, by which charge neutrality causes the total electrostatic energy to be an extensive quantity. On the other hand, our data for 2D indicate that the total electrostatic energy is nonextensive. We were intrigued by these results on quenched 2D lattices, and as a check we evaluated numerically the total electrostatic energy (plus background energy) for an exact triangular Wigner lattice of up to $N=10\,000$ electrons. The results confirm that the total electrostatic energy is really non-extensive, and there seems to be no thermodynamic limit in 2D.

At constant β^2 the Darwin lowering of energy is smaller for larger N systems in 2D. This can also be inferred from the observation made in Sec. III A that the fraction of hot electrons goes down with increasing N. Thus our results indicate that as $\lim N\to\infty$ at constant electron density the Darwin lowering vanishes. This conclusion holds for harmonically confined systems for which β_c^2 is almost independent of N and hence different sized systems can be compared at constant β^2.

The magnetic lowering does not decrease with large N in 3D, which is suggestive that the effect could survive in a proper thermodynamic limit. In a certain sense, the Darwin interaction merely renormalizes the electronic charge. But this would interfere with the cancellation of the background charge and hence jeopardize the thermodynamic limit [33]. We feel that more numerical and analytical work is needed to resolve the question of the thermodynamic limit for the Darwin Lagrangian in 3D.

ACKNOWLEDGMENTS

We acknowledge discussions with A. Castelo, F. C. Alcaraz, and J. P. Rino. J. De Luca acknowledges Fapesp, Proc. No. 96/06479-9 and CNPQ Proc. No. 301243/94-8(NV) and V. Mehra acknowledges Fapesp, Proc. No. 98/0947-0.

[1] J. De Luca, A.J. Lichtenberg, and M.A. Lieberman, Chaos **5**, 283 (1995).
[2] J. De Luca, A.J. Lichtenberg, and S. Ruffo, Phys. Rev. E **60**, 3781 (1999).
[3] A. Compagner, C. Bruin, and A. Roesle, Phys. Rev. A **39**, 5989 (1989).
[4] H.A. Posch, H. Narnhofer, and W. Thirring, Phys. Rev. A **42**, 1880 (1990).
[5] W. Thirring and H.A. Posch, Phys. Rev. E **48**, 4333 (1993).
[6] M. Antoni and S. Ruffo, Phys. Rev. E **52**, 2361 (1995).
[7] H. Essen, Phys. Rev. E **53**, 5228 (1996); **56**, 5858 (1997).
[8] H. Essen, Phys. Scr. **40**, 789 (1989).
[9] H. Essen, J. Phys. A **32**, 2297 (1999).
[10] K.E. Brenan, S. L. Campbell, and L. R. Petzold, *Numerical Solution of Initial-Value Problems in Differential-Algebraic Equations* (Elsevier, New York, 1989).
[11] M.P. Allen and D.J. Tildesley, *Computer Simulation of Liquids* (Claredon, Oxford, 1987).
[12] C.G. Darwin, Philos. Mag. **39**, 537 (1920).
[13] G. Breit, Phys. Rev. **34**, 553 (1929); **39**, 616 (1932).
[14] J.D. Jackson, *Classical Electrodynamics*, 2nd ed. (Wiley, New York, 1975).
[15] C.W. Nielson and H.R. Lewis, in *Methods in Computational Physics*, edited by J. Kileen (Academic Press, New York, 1976), Vol. 16, pp. 367–388.
[16] A.N. Kaufman and T. Soda, Phys. Rev. **136**, A1614 (1964).
[17] D.Q. Ding, L.C. Lee, and D.W. Swift, J. Geophys. Res. **97**, 8453 (1992), and references therein.
[18] W. Appel and A. Alastuey, Physica A **252**, 238 (1998).
[19] J. De Luca, Phys. Rev. Lett. **80**, 680 (1998); Phys. Rev. E **58**, 5727 (1998).
[20] R.N. Hill, in *Relativistic Action-at-a-Distance: Classical and Quantum Aspects*, edited by J. Llosa, Lecture Notes in Physics Vol. 162 (Springer, New York, 1982), p. 104.
[21] J. Krizan and P. Havas, Phys. Rev. **128**, 2916 (1962).
[22] J.L. Anderson, *Principles of Relativity Physics* (Academic, New York, 1967), p. 225.
[23] L. Page, Phys. Rev. **11**, 376 (1918); R. Neiden Hill, J. Math. Phys. **8**, 201 (1972).
[24] D.H.E. Dubin and T.M. O'Neil, Rev. Mod. Phys. **71**, 87 (1999).
[25] V.M. Bedanov and F.M. Peeters, Phys. Rev. B **49**, 2667 (1994).

[26] L. Candido, J.P. Rino, N. Studart, and F. Peeters, J. Phys.: Condens. Matter **10**, 11 627 (1998).
[27] J.H. Van Vleck, *The Theory of Electric and Magnetic Susceptibilities* (Clarendon, Oxford, 1932), Chap. IV.
[28] S. Ichimaru, *Statistical Plasma Physics* (Addison-Wesley, Reading, MA, 1992), p. 6.
[29] V.I. Arnold, *Mathematical Methods of Classical Mechanics* (Springer-Verlag, New York, 1978).
[30] E.G. Bessonov, e-print physics/9902065.
[31] P.M. Morse and H. Feshbach, *Methods of Theoretical Physics* (McGraw-Hill, New York, 1953), Part II, p. 1267.
[32] E. Hairer and G. Wanner, *Solving Ordinary Differential Equations II*, 2nd ed. (Springer, Berlin, 1996).
[33] D. Ruelle, Helv. Phys. Acta **36**, 183 (1963).